Modeling of bending-torsion couplings in active-bending structures. Application to the design of elastic gridshell.

Thèse n. xxxxx
présenté le 01 décembre 2017
à l'Ecole des Ponts ParisTech
laboratoire Navier
Université Paris-Est

pour l'obtention du grade de Docteur ès Sciences
par

Lionel du Peloux

acceptée sur proposition du jury:

Prof Name Surname, président du jury
Prof Name Surname, directeur de thèse
Prof Name Surname, rapporteur
Prof Name Surname, rapporteur
Prof Name Surname, rapporteur

Paris, Ecole des Ponts ParisTech, 2016

Contents

Contents i

List of Figures iii

List of Tables v

4 Elastic rod : variational approach 1

4.1 Introduction . . . 1
4.1.1 Overview . . . 2
4.1.2 Contributions . . . 2
4.1.3 Related work . . . 2
4.2 Kirchhoff rod . . . 3
4.2.1 Description of the motion . . . 3
4.2.2 Inextensibility assumption . . . 4
4.2.3 Euler-Bernouilli assumption . . . 4
4.2.4 Governing equations . . . 4
4.2.5 Curvatures and twist . . . 5
4.2.6 Elastic energy . . . 5
4.3 Curve-angle representation . . . 6
4.3.1 Zero-twisting frame . . . 7
4.4 Strains . . . 8
4.4.1 Axial strain . . . 8
4.4.2 Bending strain . . . 8
4.4.3 Torsional strain . . . 9
4.5 Elastic energy . . . 9
4.6 Quasistatic assumption . . . 10
4.7 Energy gradient with respect to θ : moment of torsion . . . 10
4.7.1 Derivative of material directors with respect to θ . . . 10
4.7.2 Derivative of the material curvatures vector with respect to θ . . . 10
4.7.3 Computation of the moment of torsion . . . 11
4.8 Energy gradient with respect to x : internal forces . . . 12
4.8.1 Derivative of material directors with respect to x . . . 12
4.8.2 Derivative of the material curvatures vector with respect to x . . . 18

4.8.3 Computation of the forces acting on the centerline 19
4.9 Conclusion 22
4.10 References 23

List of Figures

4.1 Curve-angle representation of the rod 7
4.2 Repères de Frenet attachés à γ. 14
4.3 F is obtained by rotating $\tilde{F}_\epsilon$ around $\boldsymbol{t}$ of an angle Ψ_ϵ. 15
4.4 $\tilde{F}_\epsilon$ is obtained by parallel tranpsporting F_ϵ from $\boldsymbol{t}_\epsilon$ to $\boldsymbol{t}$. This operation could be seen as a rotation around $\boldsymbol{t}_\epsilon \times \boldsymbol{t}$ of an angle α_ϵ. 15

List of Tables

4 Elastic rod : variational approach

This chapter should be understood as an extension of the work initiated by Tayeb 2015 [1] and published by du Peloux et al. 2015 [2] and Lefevre et al. 2017 [3].

4.1 Introduction

Elastic gridshells are lightweight structures made of interconnected slender beams (see **??**). Modeling the deformation process of such structures is complex as it involves to take account for the geometric non linearities induced by the large displacements and rotations of the grid. More over, the large number of connexions and the coupling between flexion and torsion highly increase the complexity of the analysis.

To facilitate the design process of elastic gridshells, architects and engineers need a dedicated numerical tool that provide a good level of interactivity – which means that numerical computations must converge within a reasonable time, if not in real time – and gives deep insights on the geometry and on the mechanical behavior of the grid. This tool must be able to model complex connexions and various types of support conditions to enhance the user experience during the formfinding stage and to improve his ability to explore the space of constructible shapes.

In this chapter, our goal is to develop a beam model suitable for the modeling of grids of interconnected slender beams in order to study the mechanics of elastic gridshells. For such beams, Kirchhoff's theory of rods is considered to be appropriate. We follow recent advances in the field of computer graphics about hair modeling [4] to build a reduced degrees of freedom rod model thanks to an appropriate curve-angle representation. This representation is based on a relevant curve framing, namely the Bishop frame presented in **??**. The rod will be considered inextensible. Moreover, it will be assumed that cross-sections remain normal to the rod centerline. The internal forces and moments acting on the rod will be deduced from the differentiation of the elastic energy of the beam with respect to

the degrees of freedom of the system.

This chapter is devoted to the development of the beam model. The formulation of a discrete element and its implementation in a numerical solver are treated in a dedicated chapter (see **??**).

4.1.1 Overview

We begin this chapter by establishing a representation for any geometric configuration of a Kirchhoff rod (see §4.2) based on a curve-angle description. This representation is

4.1.2 Contributions

- We consolidate the mathematical development of the beam model by introducing the Fréchet and Gateaux derivatives in function spaces.
- We clarify the independence of the the rotational degree of freedom (θ) with respect to translational degrees of freedom ($\boldsymbol{x}$).
- We factorize the expressions of the internal forces and moments by reusing the quasi-static assumption.
- We identify the contributions of axial and shear forces, bending and torsion moments in the expressions of internal forces and moments.
- We prove the equivalence with the shear force obtained from the dynamical equations of Kirchhoff.
- We suggest that the dynamical Kirchhoff equations should be a more straight forward starting point to build up similar theories.

4.1.3 Related work

Bergou et al. 2008 [4] present a discrete treatment of adapted framed curves, parallel transport, and holonomy. Based on this framework they propose a curve-angle representation of the geometric configuration of slender rods. In this representation, the orientation of the material frame is established with respect to the Bishop frame by a single scalar angle. Upon this representation they build a mechanical model for slender elastic rods with anisotropic cross-section and arbitrary rest configuration. In the dynamic the centerline is treated explicitly and material frames are treated as quasistatic. Bergou et al. 2010 [5] improve there previous model for the modeling of viscous threads.

Nabaei 2014 [6] implements the model developed by [4] in IPOPT, an interior point optimizer, to solve the static equilibrium of simply connected systems of twisted elastica.

Tayeb 2015 [1], du Peloux et al. 2015 [2] and Lefevre et al. 2017 [3] follow [4] to model grids of interconnected slender beams. They implement their model in a dynamic relaxation

solver to formfind elastic gridshells. They formulate a special connexion.

[7]. [8], [9], [10], [11]

Bertail Spilmann Hose Pour intro : [12]

4.2 Kirchhoff rod

Kirchhoff's theory of rods is presented thoroughly in the next chapter (see **??**). In this chapter, although the assumptions are not exactly the ones made by Kirchhoff in his theory, we will stick to this denomination as introduced by [4]. In the present theory we will assume that :

- the rod is inextensible,
- cross-sections remain plane,
- cross-sections remain perpendicular to the centerline,
- the material deforms elastically.

4.2.1 Description of the motion

We introduce a curvilinear coordinate system to describe the motion of our Kirchhoff rod. It is composed of a parametric space curve, called the *centerline*, equipped with a moving frame, called the *material frame*.

Deformed configuration

The actual geometric configuration of the rod is described by its centerline $\boldsymbol{x}(s)$ and its cross-sections. The centerline is a space curve parameterized by its arc length, denoted s. Cross-sections orientation are followed along the centerline by a material frame $\{\boldsymbol{d}_3(s), \boldsymbol{d}_1(s), \boldsymbol{d}_2(s)\}$ which is an adapted orthonormal moving frame aligned with the principal axes of inertia of the cross-section.

Recall from **??** that *adapted* means that the material frame is aligned with the tangent vector of the centerline :

$$\boldsymbol{d}_3(s) = \boldsymbol{x}'(s) = \boldsymbol{t}(s) \tag{4.1}$$

Here, the prime symbol denotes the derivation with respect to the arc length parameter s. Recall also from **??** that $\|\boldsymbol{x}'(s)\| = 1$ because $\boldsymbol{x}$ is parametrized by arc length.

Stress-free configuration

Among all the possible geometric configurations of the rod we identify the *stress-free configuration* or *rest configuration*, that is the configuration in which the rod is stress-free under no external forces and moments applied top it (loads, supports, ...). This configuration is crucial as the elastic energy of a rod in a given configuration relies on both its actual and rest configuration.

Hereinafter, the symbols referring to this configuration will be denoted with an overbar (e.g. $\bar{\boldsymbol{x}}(s)$).

4.2.2 Inextensibility assumption

As explained by Audoly et al. 2010 [13], based on a scaling argument, two cases arise for slender beams : either the centerline stretches and bending and twisting forces become negligible compared to axial forces ; either the centerline remains inextensible. As we are not interested in the first case – in which the beam would behave like a cable, mainly in tension – we will assume that the rod is effectively inextensible.[1]

Remark that the previous description (see §4.2.1) is only valid for inextensible rods. Indeed, for an inextensible rod the centerline does not stretches and the arc length parameter for the rest configuration is also a valid arc length parameter for any other configuration.[2]

Hereinafter, the length of the rod will be denoted L and the arc length s will vary in $[0, L]$, with no loss of generality.

4.2.3 Euler-Bernouilli assumption

Strains are supposed to remain small so that the cross-sections remain plane and the material frame remain orthonormal and adapted to the centerline during the motion of the rod. In other words the cross-sections undergo rigid body motions.[3]

4.2.4 Governing equations

Thus, differentiating the conditions of orthonormality of the material frame (see **??**) leads to the following system of differential equations governing the evolution of the *material directors* $\{\boldsymbol{d}_3(s), \boldsymbol{d}_1(s), \boldsymbol{d}_2(s)\}$ along the centerline :

$$\begin{bmatrix} \boldsymbol{d}_3'(s) \\ \boldsymbol{d}_1'(s) \\ \boldsymbol{d}_2'(s) \end{bmatrix} = \begin{bmatrix} 0 & \kappa_2(s) & -\kappa_1(s) \\ -\kappa_2(s) & 0 & \tau(s) \\ \kappa_1(s) & -\tau(s) & 0 \end{bmatrix} \begin{bmatrix} \boldsymbol{d}_3(s) \\ \boldsymbol{d}_1(s) \\ \boldsymbol{d}_2(s) \end{bmatrix} \tag{4.2}$$

[1] For a complete treatment of the question of inextensibility refer to **??** in **??**.
[2] For a complete treatment of the question of reparametrization refer to **??** in **??**.
[3] For a complete treatment of this point in Kirchhoff's theory refer to **??** in **??**.

These equations can be formulated with the *Darboux vector* of the chosen material frame, which represents the angular velocity vector of the frame along $\boldsymbol{x}(s)$:

$$\boldsymbol{d}_i'(s) = \boldsymbol{\Omega}_m(s) \times \boldsymbol{d}_i(s) \tag{4.3a}$$

$$\boldsymbol{\Omega}_m(s) = \begin{bmatrix} \tau(s) \\ \kappa_1(s) \\ \kappa_2(s) \end{bmatrix} \tag{4.3b}$$

where $\tau(s)$, $\kappa_1(s)$ and $\kappa_2(s)$ represent the components of the angular velocity of the material frame around its axes $\boldsymbol{d}_3(s)$, $\boldsymbol{d}_1(s)$ and $\boldsymbol{d}_2(s)$ when it travels along the centerline at unit speed.[4]

4.2.5 Curvatures and twist

The material curvatures are denoted $\kappa_1(s)$ and $\kappa_2(s)$ and represent the rod's flexion in the principal planes respectively normal to $\boldsymbol{d}_1(s)$ and $\boldsymbol{d}_2(s)$.The material twist is denoted $\tau(s)$ and represents the section's rate of rotation around $\boldsymbol{d}_3(s)$. Those scalar functions measure directly the strain as defined in Kirchhoff's theory.[5]

Recall from **??** that the Frenet frame $\{\boldsymbol{t}(s), \boldsymbol{n}(s), \boldsymbol{b}(s)\}$ defines the osculating plane and the curvature (κ) of a spatial curve :

$$\boldsymbol{t}'(s) = \boldsymbol{x}''(s) = \kappa(s) \cdot \boldsymbol{n}(s) \tag{4.4a}$$

$$\kappa(s) = \|\boldsymbol{t}'(s)\| = \|\boldsymbol{x}''(s)\| \tag{4.4b}$$

$$\boldsymbol{b}(s) = \boldsymbol{t}(s) \times \boldsymbol{n}(s) \tag{4.4c}$$

To describe the osculating plane in which lies the bending part of the deformation we rely on the *curvature binormal* introduced previously in **??** :

$$\boldsymbol{\kappa b}(s) = \boldsymbol{t}(s) \times \boldsymbol{t}'(s) = \kappa(s) \cdot \boldsymbol{b}(s) \tag{4.5}$$

The curvature binormal is the vector of direction $\boldsymbol{b}(s)$ and norm $\kappa(s)$. At each point of arc length s the osculating plane is normal to $\boldsymbol{\kappa b}(s)$.

4.2.6 Elastic energy

Kirchhoff's theory assigns an elastic energy to beams according to their strain [13]. In this theory, a beam is supposed to be inextensible. Thus the elastic energy ($\mathcal{E}$) only accounts for torsion and bending behaviors and is given by :

$$\mathcal{E} = \frac{1}{2}\int_0^L EI_1(\kappa_1 - \overline{\kappa}_1)^2 + EI_2(\kappa_2 - \overline{\kappa}_2)^2 ds + \frac{1}{2}\int_0^L GJ(\tau - \overline{\tau})^2 ds \tag{4.6}$$

[4] See **??** in **??** for a geometric interpretation of these rates of rotation.

[5] For a complete treatment of the definition of material strains refer to **??** in **??**.

Here, $\overline{\kappa}_1$, $\overline{\kappa}_2$ and $\overline{\tau}$ denote the natural material curvatures and material twist of the rod in the rest configuration. E and G are the elastic and shear modulus of the material. I_1 and I_2 are the moments of inertia of the cross-section. J is the torsion constant of the cross-section.

4.3 Curve-angle representation

In the previous paragraph we have shown how the elastic energy of a rod can be computed with respect to the position of its centerline and the orientation of its cross-sections. This representation can be naturally described with six degrees of freedom (6-DOFs) :[6]

- 3-DOFs for the position of the centerline,
- and 3-DOFs for the orientation of the cross-sections.

Following Bergou et al. 2008 [4] we introduce a reduced coordinate formulation of the rod that accounts for only 4-DOFs :

- 3-DOFs for the position of the centerline,
- and only 1-DOF for the orientation of the cross-sections.

This reduction of the number of DOFs relies on the choice of a suitable reference frame, namely a Bishop (or zero-twisting) frame denoted $\{\boldsymbol{t}(s), \boldsymbol{u}(s), \boldsymbol{v}(s)\}$. Recall fom **??** in **??** that this reference frame is adapted to the centerline and exhibits a null angular velocity around the centerline's tangent vector, which means :

$$\boldsymbol{u} \cdot \boldsymbol{v}' = \boldsymbol{u}' \cdot \boldsymbol{v} = 0 \tag{4.7}$$

The Bishop frame only depends on $\boldsymbol{x}$, the geometry of the centerline, depending on the choice of an initial condition. This reference frame is obtained alla along the curve by propagating a given initial frame (at $s = 0$) with parallel transport (see **??**). By construction, this reference frame evolves along the curve at angular velocity :

$$\boldsymbol{\Omega}_b(s) = \boldsymbol{\kappa}\boldsymbol{b} = \boldsymbol{t} \times \boldsymbol{t}' \tag{4.8}$$

Remark that $\boldsymbol{\Omega}_b(s)$ only depends on the centerline and is well defined even when the curvature vanishes (whereas the Frenet frame would be undefined when the curvature vanishes). In that case the parallel transport operator becomes the rotation of null angle, which is still a valid transformation.

Thus, cross section orientations $\{\boldsymbol{d}_3(s), \boldsymbol{d}_1(s), \boldsymbol{d}_2(s)\}$ can be tracked only by the measure of an angle θ from this reference frame denoted $\{\boldsymbol{d}_3(s), \boldsymbol{u}(s), \boldsymbol{v}(s)\}$ (Figure 5).

[6] This is the usual choice where the orientation of the material frame is parametrized by a rotation matrix, or equivalently a quaternion.

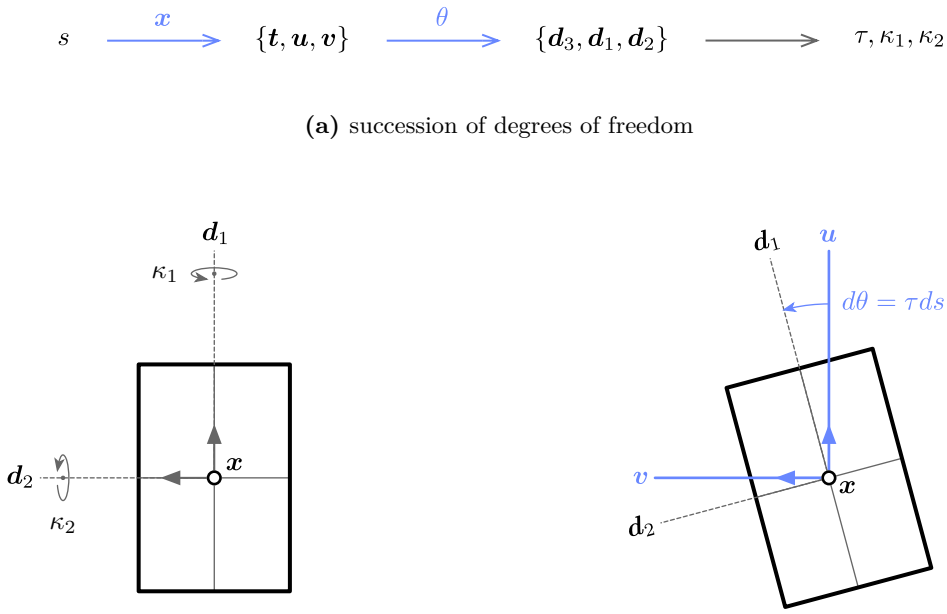

(a) succession of degrees of freedom

(b) bending strains

(c) angular deviation

Figure 4.1 – Curve-angle representation of the rod. The orientation of the material frame is established from the reference frame by its angular deviation $\theta(s)$.

Note that an alternative solution could be to parameterize the global rotations of local material frame and to compute the rotation needed to align two successive frames along the curve's tangent.

Ici, expliquer la succession des dépendances : les vecteurs matériaux dépendent du repère de bishop par la seule variable theta. Le repère de bishop quand à lui est entièrement déterminé (au choix d'une constante de départ près) par la donnée de la centerline x.

Faire un schéma explicatif.

quid du transport parallèle en temps et non en espace ?

4.3.1 Zero-twisting frame

Zero-twisting frame, also known as Bishop frame, was introduced by Bishop in 1964. Bishop remarked that there was more than one way to frame a curve [14]. Indeed, for a given curve, any orthonormal moving frame would satisfy the following differential equations,

where $k_1(s)$, $k_2(s)$ and $\tau(s)$ are scalar functions that define completely the moving frame :

$$\begin{bmatrix} \mathbf{e_3}'(s) \\ \mathbf{e_1}'(s) \\ \mathbf{e_2}'(s) \end{bmatrix} = \begin{bmatrix} 0 & k_2(s) & -k_1(s) \\ -k_2(s) & 0 & \tau(s) \\ k_1(s) & -\tau(s) & 0 \end{bmatrix} \begin{bmatrix} \mathbf{e_3}(s) \\ \mathbf{e_1}(s) \\ \mathbf{e_2}(s) \end{bmatrix} \tag{4.9}$$

For instance, a Frenet frame $\{\boldsymbol{t}(s), \boldsymbol{n}(s), \boldsymbol{b}(s)\}$ is a frame which satisfies $k_1(s) = 0$. Note that this frame suffers from major disadvantages : it is undefined where the curvature vanishes and it flips at inflexion points. A Bishop frame $\{\boldsymbol{t}(s), \boldsymbol{u}(s), \boldsymbol{v}(s)\}$ is a frame which satisfies $\tau(s) = 0$. By construction, this frame has no angular velocity (i.e. no twist) around the curve's tangent ($\boldsymbol{u} \cdot \boldsymbol{v}' = \boldsymbol{u}' \cdot \boldsymbol{v} = 0$). Its evolution along the curve is described by the corresponding Darboux vector : $\boldsymbol{\Omega}_b(s) = \boldsymbol{\kappa b} = \boldsymbol{t} \times \boldsymbol{t}'$.

4.4 Strains

4.4.1 Axial strain

There is no axial strain to be considered as far as the rod is supposed to be unstretchable.

Remark that the inextensibility hypothesis implies that any admissible perturbation ($\lambda \boldsymbol{h}_x$) of the rod's centerline ($\boldsymbol{x}$) is locally orthogonal to the centerline itself. Indeed, at each arc length s an inextensible rod must satisfies :

$$\|\boldsymbol{x}'\| = \|(\boldsymbol{x} + \lambda \boldsymbol{h}_x)'\| = 1 \Rightarrow \boldsymbol{d}_3 \cdot \boldsymbol{h}_x' = -\tfrac{\lambda^2}{2}\|\boldsymbol{h}_x'\|^2 = o(\lambda) \simeq 0 \tag{4.10}$$

In other words, this means that the same arc length parametrization can be used to locate beam sections along the centerline along the deformation path. This would not be the case if the centerline would shorten or stretch out during its deformation. It is worth to mention here that this property ($\boldsymbol{d}_3 \cdot \boldsymbol{h}_x' = 0$) will be used several times in the following sections.

4.4.2 Bending strain

Let's compute the bending strains κ_1 and κ_2 regarding the geometric configuration of the rod. Remark that :

$$\boldsymbol{\kappa b} \cdot \boldsymbol{d}_1 = (\boldsymbol{d}_3 \times \boldsymbol{d}_3') \cdot \boldsymbol{d}_1 = (\boldsymbol{d}_1 \times \boldsymbol{d}_3) \cdot \boldsymbol{d}_3' = -\boldsymbol{d}_2 \cdot \boldsymbol{d}_3' = \kappa_1 \tag{4.11a}$$

$$\boldsymbol{\kappa b} \cdot \boldsymbol{d}_2 = (\boldsymbol{d}_3 \times \boldsymbol{d}_3') \cdot \boldsymbol{d}_2 = (\boldsymbol{d}_2 \times \boldsymbol{d}_3) \cdot \boldsymbol{d}_3' = \boldsymbol{d}_1 \cdot \boldsymbol{d}_3' = \kappa_2 \tag{4.11b}$$

That is to say $\boldsymbol{\kappa b}$ is orthogonal to $\boldsymbol{d}_3$:

$$\boldsymbol{\kappa b} = \kappa_1 \boldsymbol{d}_1 + \kappa_2 \boldsymbol{d}_2 \tag{4.12}$$

Thus, the vector of material curvatures ($\boldsymbol{\omega}$) expressed on material frame axes $\{\boldsymbol{d}_1(s), \boldsymbol{d}_2(s)\}$ is defined as :

$$\boldsymbol{\omega} = \begin{bmatrix} \kappa_1 \\ \kappa_2 \end{bmatrix} = \begin{bmatrix} \boldsymbol{\kappa b} \cdot \boldsymbol{d}_1 \\ \boldsymbol{\kappa b} \cdot \boldsymbol{d}_2 \end{bmatrix} = \begin{bmatrix} -\boldsymbol{x}'' \cdot \boldsymbol{d}_2 \\ \boldsymbol{x}'' \cdot \boldsymbol{d}_1 \end{bmatrix} \tag{4.13}$$

4.4.3 Torsional strain

Let's compute the twist or torsional strain τ regarding the geometric configuration of the rod. Decomposing the material frame on the bishop frame gives :

$$\begin{bmatrix} \boldsymbol{d}_1 \\ \boldsymbol{d}_2 \end{bmatrix} = \begin{bmatrix} \cos\theta & \sin\theta \\ -\sin\theta & \cos\theta \end{bmatrix} \begin{bmatrix} \boldsymbol{u} \\ \boldsymbol{v} \end{bmatrix} \tag{4.14}$$

Thus, the twist can be identified directly as the variation of θ along the curve :

$$\tau = \boldsymbol{d}_1' \cdot \boldsymbol{d}_2 = (\theta' \boldsymbol{d}_2 + \boldsymbol{\kappa b} \times \boldsymbol{d}_1) \cdot \boldsymbol{d}_2 = \theta' + \boldsymbol{d}_3 \cdot \boldsymbol{\kappa b} = \theta' \tag{4.15}$$

Note that the Frenet frame does not lead to a correct evaluation of the twist.

4.5 Elastic energy

Introducing $\boldsymbol{\omega}$ and θ, the elastic energy can be rewritten as follow :

$$\mathcal{E} = \mathcal{E}_b + \mathcal{E}_t = \tfrac{1}{2} \int_0^L (\boldsymbol{\omega} - \bar{\boldsymbol{\omega}})^T B (\boldsymbol{\omega} - \bar{\boldsymbol{\omega}}) ds + \tfrac{1}{2} \int_0^L \beta (\theta' - \bar{\theta}')^2 ds \tag{4.16}$$

Where B is the bending stiffness matrix along the principal axes of inertia and β is the torsional stiffness :

$$B = \begin{bmatrix} EI_1 & 0 \\ 0 & EI_2 \end{bmatrix} \quad , \quad \beta = GJ \tag{4.17}$$

Recall that the rod is supposed to be inextensible in Kirchhoff's theory. Thus, there is no stretching energy associated with an axial strain. However, this constraint may be enforced via a penalty energy, which in practice is somehow very similar as considering an axial stiffness into the beam's

Remark that the twisting energy ($\mathcal{E}_t$) only depends on θ and is independent regarding $\boldsymbol{x}$ while the bending energy ($\mathcal{E}_b$) depends on both θ and $\boldsymbol{x}$ variables (remind that κ_1 and κ_2 are the projections of $\boldsymbol{\kappa b}$ over $\boldsymbol{d}_1$ over $\boldsymbol{d}_2$). Thus, a coupling between bending and twisting appears as the minimum of the whole elastic energy is not necessarily reached for concomitant minimums of bending and twisting energies.

From this energy formulation, an interesting an well-known result on elastic rods could be highlighted : "torsion is uniform in an isotropic rod that is straight in its rest configuration" [15].

Indeed, let's take an isotropic rod ($EI_1 = EI_2 = EI$) that is straight in its rest configuration ($\overline{\kappa}_1 = \overline{\kappa}_2 = 0$). Then, the bending energy becomes : $\mathcal{E}_b = EI_1\kappa_1^2 + EI_2\kappa_2^2 = EI\kappa^2$, and consequently doesn't depends on θ anymore. The curvature of the rod only depends on the geometry of its centerline ($\kappa = ||\boldsymbol{\kappa b}|| = ||\boldsymbol{x}' \times \boldsymbol{x}''||$). Thus, there is no more coupling between bending and twisting and the global minimum of elastic energy is reached while minimizing separately bending an twisting energies. That is to say the geometry of the rod ($\boldsymbol{x}$) is the one that minimized $\mathcal{E}_b$. The minimum of $\mathcal{E}_t$ is zero and is achieved for a uniform twist along the centerline, only prescribed by the boundary conditions.

4.6 Quasistatic assumption

Following [4], it is relevant to assume that the propagation of twist waves is instantaneous compared to the one of bending waves. Thus, internal forces $\boldsymbol{f}^{int}$ and moment of torsion $\boldsymbol{m}^{int}$ acts on two different timescales in the rod dynamic. Thus on the timescale of action of the force $\boldsymbol{f}^{int}$ on the center line, driving the bending waves, the twist waves propagate instantaneously, so that $\forall s \in [0, L],\ \delta\mathcal{E}/\delta\theta = 0$ for the computation of $\boldsymbol{f}^{int}$. This assumption may not be enforced, as in [**Nabei2014**], but leads to simpler and faster computations.

4.7 Energy gradient with respect to θ : moment of torsion

Internal moment of torsion and forces acting on the rod are classically obtained by differentiating the potential energy of the system with respect to θ and $\boldsymbol{x}$. Here, the calculus is a bit tricky as far as the differentiation takes place in function spaces. After a brief reminder on functional derivative, the main results of the calculations of the energy derivatives are given.

4.7.1 Derivative of material directors with respect to θ

Recalling that θ and $\boldsymbol{x}$ are independant variables and that Bishop frame $\{\boldsymbol{u}, \boldsymbol{v}\}$ only depends on $\boldsymbol{x}$, the decomposition of material frame directors $\{\boldsymbol{d}_1, \boldsymbol{d}_2\}$ on Bishop frame leads directly to the following expression for the derivative of the material directors :

$$\boldsymbol{D}_\theta \boldsymbol{d}_1(s) \cdot h_\theta = \frac{d}{d\lambda}\boldsymbol{d}_1[\theta + \lambda h_\theta]\Big|_{\lambda=0} = (-\sin\theta\ \boldsymbol{u} + \cos\theta\ \boldsymbol{v}) \cdot h_\theta = \boldsymbol{d}_2 \cdot h_\theta \tag{4.18a}$$

$$\boldsymbol{D}_\theta \boldsymbol{d}_2(s) \cdot h_\theta = \frac{d}{d\lambda}\boldsymbol{d}_2[\theta + \lambda h_\theta]\Big|_{\lambda=0} = (-\cos\theta\ \boldsymbol{u} - \sin\theta\ \boldsymbol{v}) \cdot h_\theta = -\boldsymbol{d}_1 \cdot h_\theta \tag{4.18b}$$

4.7.2 Derivative of the material curvatures vector with respect to θ

Regarding the definition of the material curvatures vector and the derivative of material directors with respect to θ, it follows immediately that :

$$\boldsymbol{D}_\theta \boldsymbol{\omega}(s) \cdot h_\theta = \frac{d}{d\lambda}\boldsymbol{\omega}[\theta + \lambda h_\theta]\Big|_{\lambda=0} = \begin{bmatrix} \boldsymbol{\kappa b} \cdot \boldsymbol{d}_2 \\ -\boldsymbol{\kappa b} \cdot \boldsymbol{d}_1 \end{bmatrix} \cdot h_\theta = -\boldsymbol{J}\boldsymbol{\omega} \cdot h_\theta \tag{4.19}$$

Where $\boldsymbol{J}$ is the matrix that acts on two dimensional vectors by counter-clockwise rotation of angle $\frac{\pi}{2}$:

$$\boldsymbol{J} = \begin{bmatrix} 0 & -1 \\ 1 & 0 \end{bmatrix} \tag{4.20}$$

4.7.3 Computation of the moment of torsion

The moment of torsion is given by the functional derivative of the potential elastic energy with respect to θ which can be decomposed according to the chaine rule :

$$\begin{aligned} \langle -m(s)\,, h_\theta \rangle = \boldsymbol{D}_\theta \mathcal{E}(s) \cdot h_\theta &= \boldsymbol{D}_\theta \mathcal{E}_b(s) \cdot h_\theta + \boldsymbol{D}_\theta \mathcal{E}_t(s) \cdot h_\theta \\ &= \boldsymbol{D}_\theta \mathcal{E}_b[\boldsymbol{\omega}[\theta]](s) \cdot h_\theta + \boldsymbol{D}_\theta \mathcal{E}_t[\theta](s) \cdot h_\theta \end{aligned} \tag{4.21}$$

Derivative of the torsion energy with respect to θ

Decomposing the previous calculus gives:

$$\begin{aligned} \boldsymbol{D}_\theta \mathcal{E}_t[\theta](s) \cdot h_\theta &= \frac{d}{d\lambda} \mathcal{E}_t[\theta + \lambda h_\theta]\Big|_{\lambda=0} \\ &= \frac{d}{d\lambda} \left(\tfrac{1}{2} \int_0^L \beta \left((\theta + \lambda h_\theta)' - \overline{\theta}' \right)^2 \, dt \right)\Big|_{\lambda=0} \\ &= \int_0^L \beta(\theta' - \overline{\theta}') \cdot h_\theta' \, dt \\ &= \left[\beta(\theta' - \overline{\theta}') \cdot h_\theta \right]_0^L - \int_0^L \left(\beta(\theta' - \overline{\theta}') \right)' \cdot h_\theta \, dt \\ &= \int_0^L \Big(\beta(\theta' - \overline{\theta}')(\delta_L - \delta_0) - \left(\beta(\theta' - \overline{\theta}') \right)' \Big) \cdot h_\theta \, dt \end{aligned} \tag{4.22}$$

Derivative of the bending energy with respect to θ

The derivative of $\mathcal{E}_b$ is obtained with the chaine rule :

$$\begin{aligned} \boldsymbol{D}_\omega \mathcal{E}_b[\boldsymbol{\omega}](s) \cdot \boldsymbol{h}_\omega &= \frac{d}{d\lambda} \mathcal{E}_b[\boldsymbol{\omega} + \lambda \boldsymbol{h}_\omega]\Big|_{\lambda=0} \\ &= \frac{d}{d\lambda} \left(\tfrac{1}{2} \int_0^L \left((\boldsymbol{\omega} + \lambda \boldsymbol{h}_\omega) - \overline{\boldsymbol{\omega}} \right)^T \boldsymbol{B} \left((\boldsymbol{\omega} + \lambda \boldsymbol{h}_\omega) - \overline{\boldsymbol{\omega}} \right) \, dt \right)\Big|_{\lambda=0} \\ &= \int_0^L (\boldsymbol{\omega} - \overline{\boldsymbol{\omega}})^T \boldsymbol{B} \cdot \boldsymbol{h}_\omega \, dt \end{aligned} \tag{4.23}$$

Finally, reminding eq 4.14 :

$$\begin{aligned} \boldsymbol{D}_\theta \mathcal{E}_b[\boldsymbol{\omega}[\theta]](s) \cdot h_\theta &= \boldsymbol{D}_\omega \mathcal{E}_b[\boldsymbol{\omega}](s) \cdot (\boldsymbol{D}_\theta \boldsymbol{\omega}[\theta](s) \cdot h_\theta) \\ &= -\int_0^L (\boldsymbol{\omega} - \overline{\boldsymbol{\omega}})^T \boldsymbol{B} \boldsymbol{J} \boldsymbol{\omega} \cdot h_\theta \, dt \end{aligned} \tag{4.24}$$

Moment of torsion

Thus, the

$$\begin{aligned}\langle -m(s)\,, h_\theta\rangle &= \boldsymbol{D}_\theta\mathcal{E}_b[\boldsymbol{\omega}[\theta]](s)\cdot h_\theta + \boldsymbol{D}_\theta\mathcal{E}_t[\theta](s)\cdot h_\theta \\ &= \int_0^L \Big(\Big(\beta(\theta'-\overline{\theta}')(\delta_L-\delta_0) - \big(\beta(\theta'-\overline{\theta}')\big)'\Big) - (\boldsymbol{\omega}-\overline{\boldsymbol{\omega}})^T\boldsymbol{B}\boldsymbol{J}\boldsymbol{\omega}\Big)\cdot h_\theta\, dt\end{aligned} \tag{4.25}$$

Finally, we can conclude on the expression of the internal moment of torsion :

$$m(s) = -\Big(\beta(\theta'-\overline{\theta}')(\delta_L-\delta_0) - \big(\beta(\theta'-\overline{\theta}')\big)'\Big) + (\boldsymbol{\omega}-\overline{\boldsymbol{\omega}})^T\boldsymbol{B}\boldsymbol{J}\boldsymbol{\omega} \tag{4.26}$$

Quasistatic hypothesis

$$\big(\beta(\theta'-\overline{\theta}')\big)' + (\boldsymbol{\omega}-\overline{\boldsymbol{\omega}})^T\boldsymbol{B}\boldsymbol{J}\boldsymbol{\omega} = 0 \tag{4.27}$$

4.8 Energy gradient with respect to x : internal forces

Internal torsional moments and forces acting on the rod are classically obtained by differentiating the potential energy of the system with respect to θ and $\boldsymbol{x}$. Here, the calculus is a bit tricky as far as the differentiation takes place in function spaces. After a brief reminder on functional derivative, the main results of the calculations of the energy derivatives are given.

paragraphe entièrment à revoir. Expliquer le cheminement. x fixe bishop et theta fixe d1,d2 par rapport à bishop. x est indépendant de theta. Seul des CL peuvent créer des couplages entre x et theta

Donc les vrais degrés de liberté du problème sont en fait les vecteurs matériels et les positions x. Se reporter à une modélisation du pb dans SO3 comme Spillmann par exemple.

Le calcul des gradients se résume donc à calculer les gradients des vecteurs matériels par rapport à des perturbations infinitésimales en x et theta. Pour theta, c'est facile. Pour kb, c'est facile. Reste la variation par rapport à x, qui est en fait la variation de bishop qu'on explique avec le writhe (défaut de fermeture de bishop sur une boucle fermée) et le transport parallèle. Le calcul se fait aisément en écrivant la double rotation et en effectuant le DL au premier ordre.

Le reste est quasiment immédiat. Reste la question des CL et des termes aux bords.

Il faut aussi se positionner par rapport à l'article de Basile. Regarder la question applied displacement vs settlement pour imposer une CL.

4.8.1 Derivative of material directors with respect to x

ici expliquer le fonctionnement de la figure

A variation of the centerline $\boldsymbol{x}$ by $\boldsymbol{\epsilon} = \lambda \boldsymbol{h}_x$ would cause a variation in the Bishop frame because parallel transport depends on the centerline itself. As far as $\boldsymbol{x}$ and θ are independent variables, this leads necessarily to a variation of the material frame. Let us denote :

- $F = \{\boldsymbol{t}, \boldsymbol{u}, \boldsymbol{v}\}$: the Bishop frame in the reference configuration ;
- $F_\epsilon = \{\boldsymbol{t}_\epsilon, \boldsymbol{u}_\epsilon, \boldsymbol{v}_\epsilon\}$: the Bishop frame in the deformed configuration ;
- $\tilde{F}_\epsilon = \{\boldsymbol{t}, \tilde{\boldsymbol{u}}_\epsilon, \tilde{\boldsymbol{v}}_\epsilon\}$: the frame obtained by parallel transporting F_ϵ back on F.

What we want to achive is to write at arc length s the Bishop frame in the deformed configuration $\{\boldsymbol{t}_\epsilon, \boldsymbol{u}_\epsilon, \boldsymbol{v}_\epsilon\}$ on the Bishop frame in the reference configuration $\{\boldsymbol{t}, \boldsymbol{u}, \boldsymbol{v}\}$ for a small perturbation ϵ of the centerline. This transformation can be decomposed in two rotations :

- $F_\epsilon \to \tilde{F}_\epsilon$: parallel transporting F_ϵ from $\boldsymbol{t}_\epsilon$ to $\boldsymbol{t}$. This is equivalent to a rotation around $\boldsymbol{t}_\epsilon \times \boldsymbol{t}$ by an angle α_ϵ.
- $\tilde{F}_\epsilon \to F$: aligning $\tilde{F}_\epsilon$ over F. This is equivalent to a rotation around $\boldsymbol{t}$ of an angle Ψ_ϵ.

Firstly, let's decompose $\{\boldsymbol{t}_\epsilon, \boldsymbol{u}_\epsilon, \boldsymbol{v}_\epsilon\}$ on the basis $\{\boldsymbol{t}, \tilde{\boldsymbol{u}}_\epsilon, \tilde{\boldsymbol{v}}_\epsilon\}$. Note that $\tilde{F}_\epsilon$ is expressed by rotating $\tilde{F}_\epsilon$ by an angle $\Psi_\epsilon[\boldsymbol{x}](s)$ around $\boldsymbol{t}$ because $\tilde{F}_\epsilon$ is obtained by parallel transporting F_ϵ from $\boldsymbol{t}_\epsilon$ to $\boldsymbol{t}$.

Calculation of Ψ_ϵ

This variation is closely related to the writhe of closed curves. As explained in [8] when parallel transporting an adapted frame around a closed curve it might not realigned with itself after one complete loop. This "lack of alignement" is directly measured by the change of writhe which can be computed with Fuller's Formula [8].

Note that the derivative of θ with respect to $\boldsymbol{x}$ can be evaluated by the change of writhe in the curve as suggested in [9]. This approach is completly equivalent.

One can also see this lack of alignement in terms of rotation. Parallel transport being a propagation of frame from $s = 0$, the cumulated rotation of Bishop frame from the deformed configuration around the initial configuration at arc length s is the cumulated angle of rotation of $\boldsymbol{u}[\boldsymbol{x} + \lambda \boldsymbol{h}_x]$ around $\boldsymbol{d}_3[\boldsymbol{x}]$. Recalling the rotation rate of $\boldsymbol{u}[\boldsymbol{x} + \lambda \boldsymbol{h}_x]$ is $\boldsymbol{\kappa b}[\boldsymbol{x} + \lambda \boldsymbol{h}_x]$ by definition of zero-twisting frame, one can write :

$$\Psi_\epsilon[\boldsymbol{x}](s) = -\int_0^s \boldsymbol{\kappa b}[\boldsymbol{x} + \lambda \boldsymbol{h}_x] \cdot \boldsymbol{d}_3[\boldsymbol{x}]\, dt \tag{4.28}$$

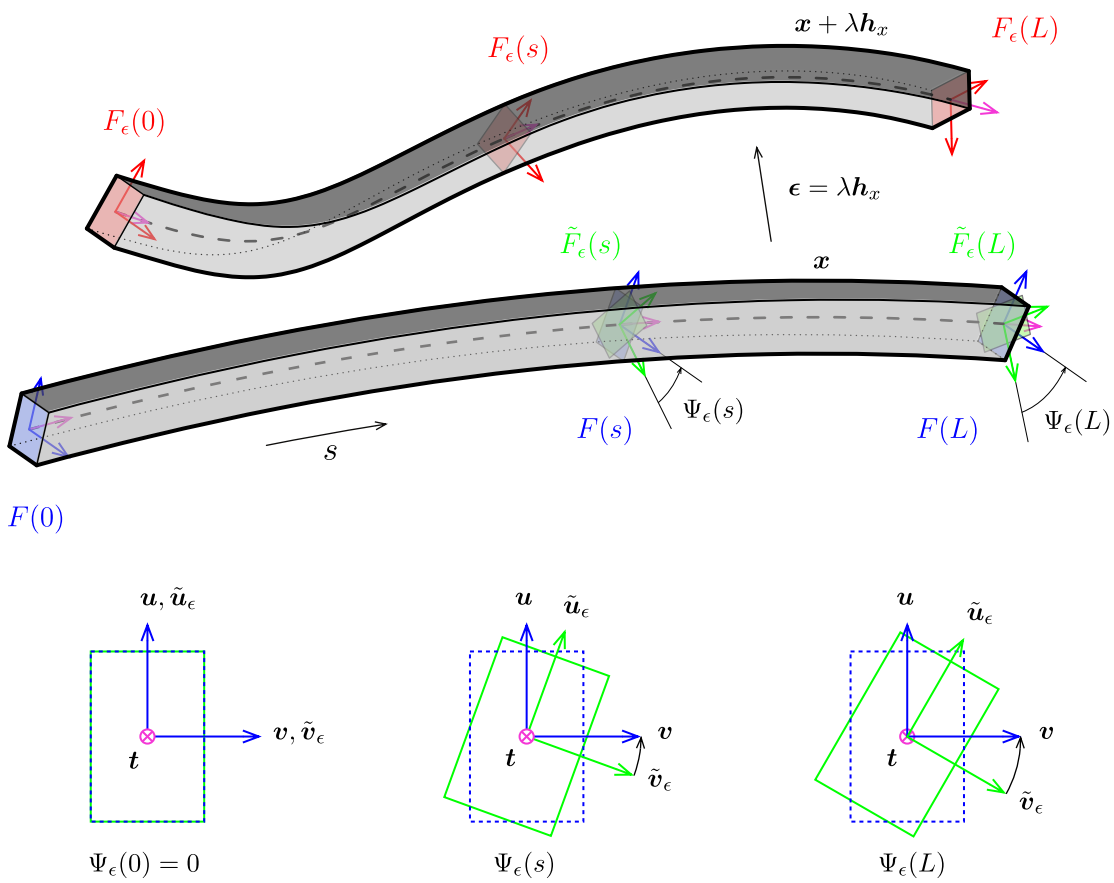

Figure 4.2 – Repères de Frenet attachés à γ.

The calculation of $\boldsymbol{\kappa b}[\boldsymbol{x}+\lambda\boldsymbol{h}_x]$ is straight forward from the curvature binormal definition :

$$\begin{aligned}\boldsymbol{\kappa b}[\boldsymbol{x}+\lambda\boldsymbol{h}_x] &= (\boldsymbol{x}+\lambda\boldsymbol{h}_x)'\times(\boldsymbol{x}+\lambda\boldsymbol{h}_x)''\\ &= \boldsymbol{\kappa b}[\boldsymbol{x}]+\lambda(\boldsymbol{x}'\times\boldsymbol{h}_x''+\boldsymbol{h}_x'\times\boldsymbol{x}'')+\lambda^2(\boldsymbol{h}_x'\times\boldsymbol{h}_x'')\\ &= \boldsymbol{\kappa b}[\boldsymbol{x}]+\lambda(\boldsymbol{x}'\times\boldsymbol{h}_x''+\boldsymbol{h}_x'\times\boldsymbol{x}'')+o(\lambda)\end{aligned} \tag{4.29}$$

Thus, reminding that $\boldsymbol{d}_3[\boldsymbol{x}]=\boldsymbol{x}'$ and $\boldsymbol{\kappa b}[\boldsymbol{x}]\cdot\boldsymbol{d}_3[\boldsymbol{x}]=0$, and using the invariance of circular product by cyclic permutation, one can express :

$$\begin{aligned}\Psi_\epsilon[\boldsymbol{x}](s) &= -\int_0^s \boldsymbol{\kappa b}[\boldsymbol{x}+\lambda\boldsymbol{h}_x]\cdot\boldsymbol{d}_3[\boldsymbol{x}]\,dt\\ &= -\lambda\int_0^s(\boldsymbol{x}'\times\boldsymbol{h}_x''+\boldsymbol{h}_x'\times\boldsymbol{x}'')\cdot\boldsymbol{x}'\,dt+o(\lambda)\\ &= -\lambda\int_0^s\boldsymbol{\kappa b}[\boldsymbol{x}]\cdot\boldsymbol{h}_x'\,dt+o(\lambda)\end{aligned} \tag{4.30}$$

By integration by parts, dropping the implicit reference to $\boldsymbol{x}$ in the notation, and denoting by δ_s and H_s the Dirac function and the Heaviside step function centered at s, $\Psi_\epsilon(s)$ could

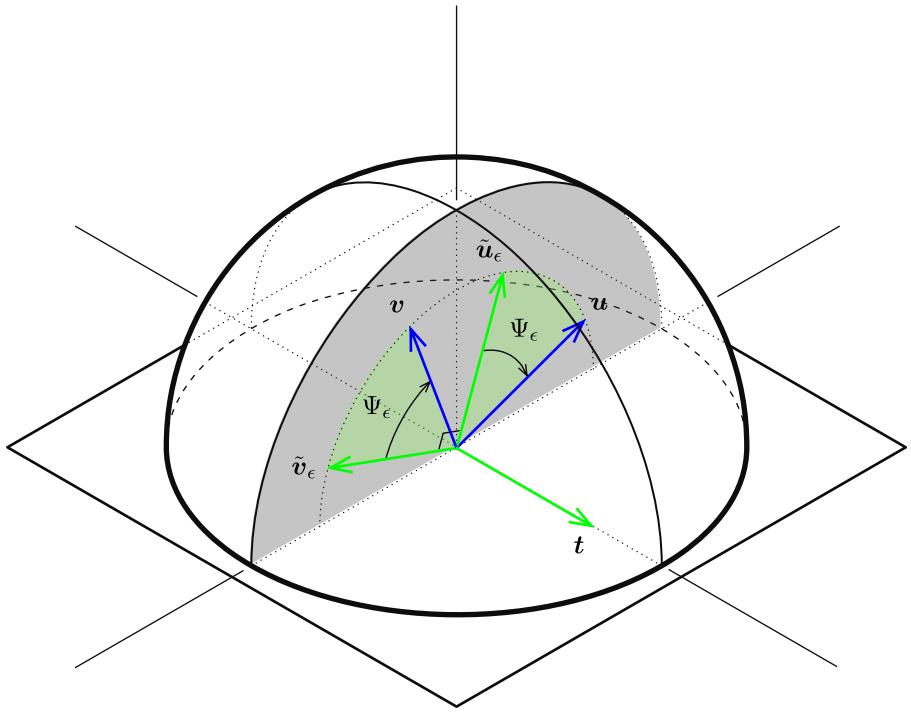

Figure 4.3 – F is obtained by rotating $\tilde{F}_\epsilon$ around $\boldsymbol{t}$ of an angle Ψ_ϵ.

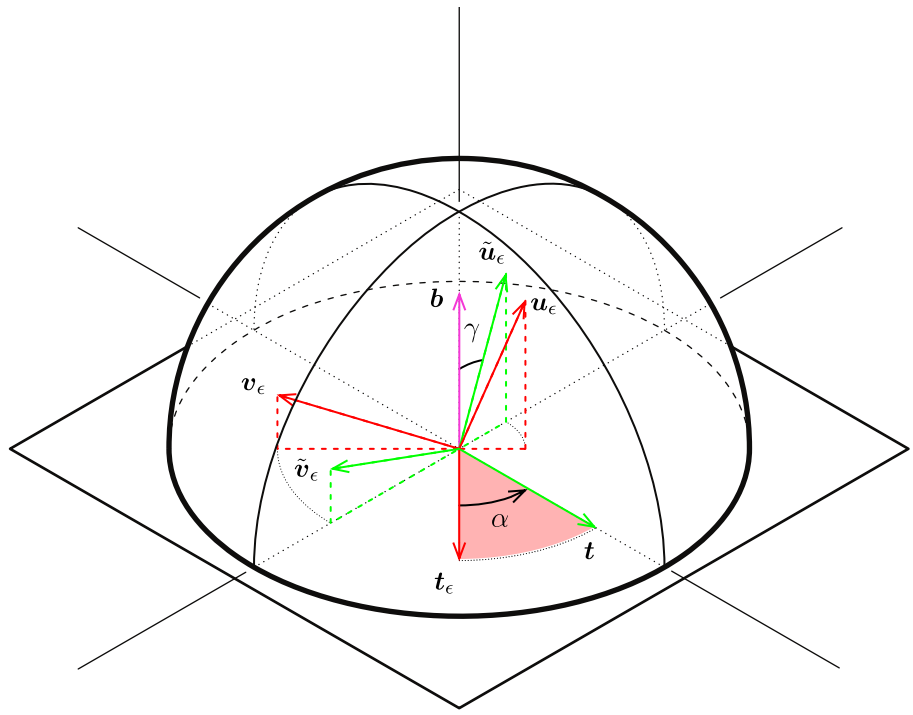

Figure 4.4 – $\tilde{F}_\epsilon$ is obtained by parallel tranpsporting F_ϵ from $\boldsymbol{t}_\epsilon$ to $\boldsymbol{t}$. This operation could be seen as a rotation around $\boldsymbol{t}_\epsilon \times \boldsymbol{t}$ of an angle α_ϵ.

be rewritten as :

$$\begin{aligned}
\Psi_\epsilon(s) &= -\lambda \int_0^s \boldsymbol{\kappa b} \cdot \boldsymbol{h}_x' \, dt + o(\lambda) \\
&= -\lambda \left(\Big[\boldsymbol{\kappa b} \cdot \boldsymbol{h}_x \Big]_0^s - \int_0^s \boldsymbol{\kappa b}' \cdot \boldsymbol{h}_x \, dt \right) + o(\lambda) \\
&= -\lambda \left(\int_0^s \left((\delta_s - \delta_0) \, \boldsymbol{\kappa b} - \boldsymbol{\kappa b}' \right) \cdot \boldsymbol{h}_x \, dt \right) + o(\lambda) \\
&= -\lambda \left(\int_0^L \left((\delta_s - \delta_0) \, \boldsymbol{\kappa b} - (1 - H_s) \boldsymbol{\kappa b}' \right) \cdot \boldsymbol{h}_x \, dt \right) + o(\lambda)
\end{aligned} \tag{4.31}$$

Note that, as expected, $\Psi_\epsilon(s)$ is in first order of λ and thus gets negligible when λ tends to zero, that is to say when the perturbation of $\boldsymbol{x}$ is infinitesimal :

$$\lim_{\lambda \to 0} \Psi_\epsilon(s) = 0 \tag{4.32}$$

$H_s \ : t \mapsto \begin{cases} 0, & t < s \\ 1, & t \geqslant s \end{cases}$ est la fonction de Heaviside.

$\delta_s \ : t \mapsto \delta(t - s)$ est la distribution de dirac centrée en s.

Calculation of α_ϵ

Recall that $\tilde{F}_\epsilon$ is obtained by parallel tranpsporting F_ϵ from $\boldsymbol{t}_\epsilon$ to $\boldsymbol{t}$. $\tilde{F}_\epsilon$ results from the rotation of F_ϵ around $\boldsymbol{b} = \boldsymbol{t}_\epsilon \times \boldsymbol{t}$ by an angle α_ϵ.

Recall from (4.10) that because the rod is supposed to be unstretchable, $\boldsymbol{t}_\epsilon$ stays collinear to $\boldsymbol{t}$ for an infinitesimal perturbation of the centerline :

$$\|\boldsymbol{t}\| = \|\boldsymbol{t}_\epsilon\| = 1 \Rightarrow (\boldsymbol{x} + \boldsymbol{\epsilon})' \cdot (\boldsymbol{x} + \boldsymbol{\epsilon})' = 1 \Leftrightarrow \boldsymbol{x}' \cdot \boldsymbol{\epsilon}' = -\tfrac{\lambda^2}{2} \|\boldsymbol{h}_x'\|^2 \tag{4.33}$$

Which leeds to :

$$\cos \alpha_\epsilon(s) = \boldsymbol{t} \cdot \boldsymbol{t}_\epsilon = \boldsymbol{x}' \cdot (\boldsymbol{x} + \boldsymbol{\epsilon})' = 1 + \boldsymbol{x}' \cdot \boldsymbol{\epsilon}' = 1 - \tfrac{\lambda^2}{2} \|\boldsymbol{h}_x'\|^2 \tag{4.34}$$

Thus, at second order in λ :

$$\cos \alpha_\epsilon = 1 - \tfrac{\lambda^2}{2} \|\boldsymbol{h}_x'\|^2 \tag{4.35a}$$

$$\sin \alpha_\epsilon = \sqrt{1 - \cos^2 \alpha_\epsilon} = \lambda \|\boldsymbol{h}_x'\| + o(\lambda^2) \tag{4.35b}$$

$$\sin^2 \alpha_\epsilon / 2 = \tfrac{\lambda^2}{4} \|\boldsymbol{h}_x'\|^2 \tag{4.35c}$$

Finally, it's possible to conclude that $\alpha_\epsilon(s)$ is in first order of λ and thus gets negligible when λ tends to zero :

$$\lim_{\lambda \to 0} \alpha_\epsilon(s) = 0 \tag{4.36}$$

Aligning $\tilde{F}_\epsilon$ towards F_ϵ

Recall that aligning $\tilde{F}_\epsilon$ over F is nothing but a rotation around $\boldsymbol{t}$ by an angle Ψ_ϵ. This leads to :

$$\tilde{\boldsymbol{u}}_\epsilon = \cos\Psi_\epsilon\, \boldsymbol{u} + \sin\Psi_\epsilon\, \boldsymbol{v} \tag{4.37a}$$
$$\tilde{\boldsymbol{v}}_\epsilon = -\sin\Psi_\epsilon\, \boldsymbol{u} + \cos\Psi_\epsilon\, \boldsymbol{v} \tag{4.37b}$$

Aligning F_ϵ towards $\boldsymbol{t}$

Recall that $\tilde{F}_\epsilon$ is obtained by parallel tranpsporting F_ϵ from $\boldsymbol{t}_\epsilon$ to $\boldsymbol{t}$. This operation could be seen as a rotation around $\boldsymbol{t}_\epsilon \times \boldsymbol{t}$ of an angle α_ϵ. Where :

$$\boldsymbol{b} = \boldsymbol{t}_\epsilon \times \boldsymbol{t} = \cos\gamma\, \tilde{\boldsymbol{u}}_\epsilon + \sin\gamma\, \tilde{\boldsymbol{v}}_\epsilon = \cos\gamma\, \boldsymbol{u}_\epsilon + \sin\gamma\, \boldsymbol{v}_\epsilon \tag{4.38}$$

Expressing F_ϵ on the basis $\tilde{F}_\epsilon$ gives for $\boldsymbol{u}_\epsilon$ and $\boldsymbol{v}_\epsilon$:

$$\boldsymbol{u}_\epsilon = \sin\gamma\, \boldsymbol{b} + \cos\gamma\, \Big(\sin\alpha_\epsilon\, \tilde{\boldsymbol{t}} + \cos\alpha_\epsilon\, (\cos\gamma\, \tilde{\boldsymbol{u}}_{\boldsymbol{\epsilon}} - \sin\gamma\, \tilde{\boldsymbol{v}}_{\boldsymbol{\epsilon}})\Big) \tag{4.39a}$$
$$\boldsymbol{v}_\epsilon = \cos\gamma\, \boldsymbol{b} + \sin\gamma\, \Big(-\sin\alpha_\epsilon\, \tilde{\boldsymbol{t}} + \cos\alpha_\epsilon\, (\sin\gamma\, \tilde{\boldsymbol{u}}_{\boldsymbol{\epsilon}} - \cos\gamma\, \tilde{\boldsymbol{v}}_{\boldsymbol{\epsilon}})\Big) \tag{4.39b}$$

Which can be rearranged in :

$$\boldsymbol{u}_\epsilon = \cos\gamma \sin\alpha_\epsilon\, \boldsymbol{t} + (\cos\alpha_\epsilon \cos^2\gamma + \cos^2\gamma)\tilde{\boldsymbol{u}}_{\boldsymbol{\epsilon}} + \sin\gamma\cos\gamma\, (1-\cos\alpha_\epsilon)\tilde{\boldsymbol{v}}_{\boldsymbol{\epsilon}} \tag{4.40a}$$
$$\boldsymbol{v}_\epsilon = -\sin\gamma \sin\alpha_\epsilon\, \boldsymbol{t} + \cos\gamma\sin\gamma\, (1-\cos\alpha_\epsilon)\tilde{\boldsymbol{u}}_{\boldsymbol{\epsilon}} + (\cos^2\gamma + \cos\alpha_\epsilon \sin^2\gamma)\tilde{\boldsymbol{v}}_{\boldsymbol{\epsilon}} \tag{4.40b}$$

Variation of Bishop frame with respect to x

Finally, one can express F_ϵ on the basis F as the composition of two rotations :

$$\boldsymbol{u}_\epsilon = \begin{bmatrix} 1 & 0 & 0 \\ 0 & \cos\Psi_\epsilon & -\sin\Psi_\epsilon \\ 0 & \sin\Psi_\epsilon & \cos\Psi_\epsilon \end{bmatrix} \begin{bmatrix} \cos\gamma\sin\alpha_\epsilon \\ 1 - 2\cos^2\gamma\sin^2\alpha_\epsilon/2 \\ 2\sin\gamma\cos\gamma\sin^2\alpha_\epsilon/2 \end{bmatrix} = \begin{bmatrix} \alpha_\epsilon\cos\gamma \\ 1 \\ \Psi_\epsilon \end{bmatrix} + o(\lambda) \tag{4.41a}$$
$$\boldsymbol{v}_\epsilon = \begin{bmatrix} 1 & 0 & 0 \\ 0 & \cos\Psi_\epsilon & -\sin\Psi_\epsilon \\ 0 & \sin\Psi_\epsilon & \cos\Psi_\epsilon \end{bmatrix} \begin{bmatrix} -\sin\gamma\sin\alpha_\epsilon \\ 2\sin\gamma\cos\gamma\sin^2\alpha_\epsilon/2 \\ 1 - 2\sin\gamma^2\sin^2\alpha_\epsilon/2 \end{bmatrix} = \begin{bmatrix} -\alpha_\epsilon\sin\gamma \\ -\Psi_\epsilon \\ 1 \end{bmatrix} + o(\lambda) \tag{4.41b}$$

Here, the expressions have been developed in first order of λ as far as α_ϵ and Ψ_ϵ it's been proofed in eq [] that those quantities tends two zero when the perturbation of the centerline is infinitesimal.

Finally, one can express the variation of material directors with respect to an infinitesimal

variation of rod's centerline :

$$\boldsymbol{u}_\epsilon = \alpha_\epsilon \cos\gamma\ \boldsymbol{t} + \boldsymbol{u} + \Psi_\epsilon \boldsymbol{v} + o(\lambda) \tag{4.42a}$$
$$\boldsymbol{v}_\epsilon = -\alpha_\epsilon \sin\gamma\ \boldsymbol{t} + \boldsymbol{v} - \Psi_\epsilon \boldsymbol{u} + o(\lambda) \tag{4.42b}$$

Variation of material frame with respect to $\boldsymbol{x}$

Recalling the expression of the material frame expressed in the reference Bishop frame, it's now easy to deduce the variation of material frame with respect to a variation of the rod's centerline :

$$\boldsymbol{d}_1[\boldsymbol{x} + \lambda \boldsymbol{h}_x] = \cos\theta\ \boldsymbol{u}_\epsilon + \sin\theta\ \boldsymbol{v}_\epsilon \tag{4.43a}$$
$$\boldsymbol{d}_2[\boldsymbol{x} + \lambda \boldsymbol{h}_x] = -\sin\theta\ \boldsymbol{u}_\epsilon + \cos\theta\ \boldsymbol{v}_\epsilon \tag{4.43b}$$

Which leads according to the previous equation to :

$$\boldsymbol{d}_1[\boldsymbol{x} + \lambda \boldsymbol{h}_x] = \boldsymbol{d}_1[\boldsymbol{x}] + \Psi_\epsilon \boldsymbol{d}_2[\boldsymbol{x}] + \alpha_\epsilon \cos(\theta - \gamma)\ \boldsymbol{t}[\boldsymbol{x}] + o(\lambda) \tag{4.44a}$$
$$\boldsymbol{d}_2[\boldsymbol{x} + \lambda \boldsymbol{h}_x] = \boldsymbol{d}_2[\boldsymbol{x}] - \Psi_\epsilon \boldsymbol{d}_1[\boldsymbol{x}] - \alpha_\epsilon \sin(\theta + \gamma)\ \boldsymbol{t}[\boldsymbol{x}] + o(\lambda) \tag{4.44b}$$

4.8.2 Derivative of the material curvatures vector with respect to x

It's know straightforward from the previous section to express the variation of the material curvatures with respect to a variation $\boldsymbol{\epsilon} = \lambda \boldsymbol{h}_x$ of $\boldsymbol{x}$ while θ remains unchanged.

$$(\boldsymbol{x} + \lambda \boldsymbol{h}_x)'' \cdot \boldsymbol{d}_1[\boldsymbol{x} + \lambda \boldsymbol{h}_x] = (\boldsymbol{x}'' + \lambda \boldsymbol{h}_x'') \cdot \Big(\boldsymbol{d}_1 + \Psi_\epsilon \boldsymbol{d}_2 + \alpha_\epsilon \cos(\theta - \gamma)\ \boldsymbol{t} + o(\lambda)\Big) \tag{4.45a}$$
$$(\boldsymbol{x} + \lambda \boldsymbol{h}_x)'' \cdot \boldsymbol{d}_2[\boldsymbol{x} + \lambda \boldsymbol{h}_x] = (\boldsymbol{x}'' + \lambda \boldsymbol{h}_x'') \cdot \Big(\boldsymbol{d}_2 - \Psi_\epsilon \boldsymbol{d}_1 - \alpha_\epsilon \sin(\theta + \gamma)\ \boldsymbol{t} + o(\lambda)\Big) \tag{4.45b}$$

Thus, recalling that $\boldsymbol{x}'' \cdot \boldsymbol{d}_3 = 0$ and that α_ϵ and Ψ_ϵ are first order quantities in λ :

$$(\boldsymbol{x} + \lambda \boldsymbol{h}_x)'' \cdot \boldsymbol{d}_1[\boldsymbol{x} + \lambda \boldsymbol{h}_x] = \boldsymbol{x}'' \cdot \boldsymbol{d}_1 + \Psi_\epsilon \boldsymbol{x}'' \cdot \boldsymbol{d}_2 + \lambda \boldsymbol{h}_x'' \cdot \boldsymbol{d}_1 + o(\lambda) \tag{4.46a}$$
$$(\boldsymbol{x} + \lambda \boldsymbol{h}_x)'' \cdot \boldsymbol{d}_2[\boldsymbol{x} + \lambda \boldsymbol{h}_x] = \boldsymbol{x}'' \cdot \boldsymbol{d}_2 - \Psi_\epsilon \boldsymbol{x}'' \cdot \boldsymbol{d}_1 + \lambda \boldsymbol{h}_x'' \cdot \boldsymbol{d}_2 + o(\lambda) \tag{4.46b}$$

Which finally leads to :

$$\boldsymbol{\omega}[\boldsymbol{x} + \lambda \boldsymbol{h}_x] = \boldsymbol{\omega}[\boldsymbol{x}] - \Psi_\epsilon \boldsymbol{J}\boldsymbol{\omega}[\boldsymbol{x}] + \lambda \begin{bmatrix} -\boldsymbol{h}_x'' \cdot \boldsymbol{d}_2 \\ \boldsymbol{h}_x'' \cdot \boldsymbol{d}_1 \end{bmatrix} + o(\lambda) \tag{4.47}$$

Reminding the expression of Ψ_ϵ computed in paragraphe[], one can express the derivative of the material curvatures vector with respect to $\boldsymbol{x}$:

$$\boldsymbol{D}_x \boldsymbol{\omega}(s) \cdot \boldsymbol{h}_x = \left(\int_0^L \left((\delta_s - \delta_0)\, \boldsymbol{\kappa}\boldsymbol{b} - (1 - H_s) \boldsymbol{\kappa}\boldsymbol{b}' \right) \cdot \boldsymbol{h}_x \, dt \right) \boldsymbol{J}\boldsymbol{\omega} + \begin{bmatrix} -\boldsymbol{d}_2{}^T \\ \boldsymbol{d}_1{}^T \end{bmatrix} \cdot \boldsymbol{h}_x'' \tag{4.48}$$

4.8.3 Computation of the forces acting on the centerline

The forces acting on the centerline are given by the functional derivative of the potential elastic energy with respect to x which can be decomposed according to the chaine rule :

$$\begin{aligned}\langle -f(s)\,, \boldsymbol{h}_x\rangle = \boldsymbol{D}_x\mathcal{E}(s)\cdot\boldsymbol{h}_x &= \boldsymbol{D}_x\mathcal{E}_b(s)\cdot\boldsymbol{h}_x + \boldsymbol{D}_x\mathcal{E}_t(s)\cdot\boldsymbol{h}_x \\ &= \boldsymbol{D}_x\mathcal{E}_b[\boldsymbol{\omega}[\boldsymbol{x}]](s)\cdot\boldsymbol{h}_x + \boldsymbol{D}_x\mathcal{E}_t[\boldsymbol{x}](s)\cdot\boldsymbol{h}_x\end{aligned} \tag{4.49}$$

Derivative of the torsion energy with respect to x

Recall that the torsion energy only depends on θ which is independent of x. Thus, $\mathcal{E}_t$ is independent of x :

$$\boldsymbol{D}_x\mathcal{E}_t[\boldsymbol{x}](s)\cdot\boldsymbol{h}_x = \frac{d}{d\lambda}\mathcal{E}_t[\boldsymbol{x}+\lambda\boldsymbol{h}_x]\Big|_{\lambda=0} = 0 \tag{4.50}$$

Derivative of the bending energy with respect to x

The derivative of $\mathcal{E}_b$ is obtained with the chaine rule :

$$\boldsymbol{D}_\omega\mathcal{E}_b[\boldsymbol{\omega}](s)\cdot\boldsymbol{h}_\omega = \frac{d}{d\lambda}\mathcal{E}_b[\boldsymbol{\omega}+\lambda\boldsymbol{h}_\omega]\Big|_{\lambda=0} = \int_0^L(\boldsymbol{\omega}-\bar{\boldsymbol{\omega}})^T\boldsymbol{B}\cdot\boldsymbol{h}_\omega\,dt \tag{4.51}$$

Finally, reminding eq 4.14 :

$$\boldsymbol{D}_x\mathcal{E}_b[\boldsymbol{\omega}[\boldsymbol{x}]](s)\cdot\boldsymbol{h}_x = \boldsymbol{D}_\omega\mathcal{E}_b[\boldsymbol{\omega}](s)\cdot(\boldsymbol{D}_x\boldsymbol{\omega}[\boldsymbol{x}](s)\cdot\boldsymbol{h}_x) = \mathcal{A}+\mathcal{B}+\mathcal{C} \tag{4.52}$$

Where :

$$\mathcal{A} = \int_0^L(\boldsymbol{\omega}-\bar{\boldsymbol{\omega}})^T\boldsymbol{B}\begin{bmatrix}-\boldsymbol{d}_2{}^T\\ \boldsymbol{d}_1{}^T\end{bmatrix}\cdot\boldsymbol{h}_x''\,dt \tag{4.53a}$$

$$\mathcal{B} = \int_{t=0}^L(\boldsymbol{\omega}-\bar{\boldsymbol{\omega}})^T\boldsymbol{B}\boldsymbol{J}\boldsymbol{\omega}\left(\int_{u=0}^L(\delta_t-\delta_0)\,\boldsymbol{\kappa}\boldsymbol{b}\cdot\boldsymbol{h}_x\,du\right)\,dt \tag{4.53b}$$

$$\mathcal{C} = \int_{t=0}^L-(\boldsymbol{\omega}-\bar{\boldsymbol{\omega}})^T\boldsymbol{B}\boldsymbol{J}\boldsymbol{\omega}\left(\int_{u=0}^L(1-H_t)\,\boldsymbol{\kappa}\boldsymbol{b}'\cdot\boldsymbol{h}_x\,du\right)\,dt \tag{4.53c}$$

Calculus of $\mathcal{A}$:

$$\mathcal{A} = \int_0^L(\boldsymbol{\omega}-\bar{\boldsymbol{\omega}})^T\boldsymbol{B}\begin{bmatrix}-\boldsymbol{d}_2{}^T\\ \boldsymbol{d}_1{}^T\end{bmatrix}\cdot\boldsymbol{h}_x''\,dt \tag{4.54}$$

Recalling the bending moment is given by :

$$\boldsymbol{M} = (\kappa_1-\bar{\kappa}_1)EI_1\boldsymbol{d}_1 + (\kappa_2-\bar{\kappa}_2)EI_2\boldsymbol{d}_2 = M_1\boldsymbol{d}_1 + M_2\boldsymbol{d}_2 \tag{4.55}$$

One can remark that :

$$(\boldsymbol{\omega} - \bar{\boldsymbol{\omega}})^T \boldsymbol{B} \begin{bmatrix} -\boldsymbol{d}_2{}^T \\ \boldsymbol{d}_1{}^T \end{bmatrix} = M_2 \boldsymbol{d}_1{}^T - M_1 \boldsymbol{d}_2{}^T = -(\boldsymbol{d}_3 \times \boldsymbol{M})^T \tag{4.56}$$

Rq : on mixe abusivement 2 formes d'écritures, matricielle et vectorielle, à cause du produit scalaire que l'on écrit tantôt sous sa forme vectorielle et parfois matricielle (à l'aide de la transposée).

Thus, $\mathcal{A}$ could be rewritten in it's vectoriel form :

$$\begin{aligned} \mathcal{A} &= -\int_0^L (\boldsymbol{d}_3 \times \boldsymbol{M}) \cdot \boldsymbol{h}_x'' \, dt \\ &= -\left[(\boldsymbol{d}_3 \times \boldsymbol{M}) \cdot \boldsymbol{h}_x'\right]_0^L + \int_0^L (\boldsymbol{d}_3 \times \boldsymbol{M})' \cdot \boldsymbol{h}_x' \, dt \\ &= -\left[(\boldsymbol{d}_3 \times \boldsymbol{M}) \cdot \boldsymbol{h}_x'\right]_0^L + \int_0^L \left((\boldsymbol{d}_3 \times \boldsymbol{M}') \cdot \boldsymbol{h}_x' + (\boldsymbol{h}_x' \times \boldsymbol{d}_3') \cdot \boldsymbol{M}\right) \, dt \end{aligned} \tag{4.57}$$

Recall that from (4.10) that $\boldsymbol{h}_x' \cdot \boldsymbol{d}_3 = 0$ and from (4.2) that $\boldsymbol{d}_3' \cdot \boldsymbol{d}_3 = 0$. Hence, $\boldsymbol{h}_x' \times \boldsymbol{d}_3'$ is colinear to $\boldsymbol{d}_3$. Or by definition $\boldsymbol{M}$ is orthogonal to $\boldsymbol{d}_3$. Thus, $(\boldsymbol{h}_x' \times \boldsymbol{d}_3') \cdot \boldsymbol{M} = 0$. Finally, after a second integration by parts :

$$\begin{aligned} \mathcal{A} &= -\left[(\boldsymbol{d}_3 \times \boldsymbol{M}) \cdot \boldsymbol{h}_x'\right]_0^L + \int_0^L (\boldsymbol{d}_3 \times \boldsymbol{M}') \cdot \boldsymbol{h}_x' \, dt \\ &= \left[(\boldsymbol{d}_3 \times \boldsymbol{M}') \cdot \boldsymbol{h}_x'' - (\boldsymbol{d}_3 \times \boldsymbol{M}) \cdot \boldsymbol{h}_x'\right]_0^L - \int_0^L (\boldsymbol{d}_3 \times \boldsymbol{M}')' \cdot \boldsymbol{h}_x \, dt \end{aligned} \tag{4.58}$$

Calculus of $\mathcal{B}$:

$$\begin{aligned} \mathcal{B} &= \int_{t=0}^L (\boldsymbol{\omega} - \bar{\boldsymbol{\omega}})^T \boldsymbol{B}\boldsymbol{J}\boldsymbol{\omega} \left(\int_{u=0}^L (\delta_t - \delta_0) \, \boldsymbol{\kappa}\boldsymbol{b} \cdot \boldsymbol{h}_x \, du \right) \, dt \\ &= -(\boldsymbol{\kappa}\boldsymbol{b} \cdot \boldsymbol{h}_x)(0) \int_{t=0}^L (\boldsymbol{\omega} - \bar{\boldsymbol{\omega}})^T \boldsymbol{B}\boldsymbol{J}\boldsymbol{\omega} \, dt + \int_{t=0}^L (\boldsymbol{\omega} - \bar{\boldsymbol{\omega}})^T \boldsymbol{B}\boldsymbol{J}\boldsymbol{\omega}\boldsymbol{\kappa}\boldsymbol{b} \cdot \boldsymbol{h}_x \, dt \end{aligned} \tag{4.59}$$

Calculus of $\mathcal{C}$:

$$\begin{aligned} \mathcal{C} &= \int_{t=0}^L -(\boldsymbol{\omega} - \bar{\boldsymbol{\omega}})^T \boldsymbol{B}\boldsymbol{J}\boldsymbol{\omega} \left(\int_{u=0}^L (1 - H_t) \, \boldsymbol{\kappa}\boldsymbol{b}' \cdot \boldsymbol{h}_x \, du \right) \, dt \\ &= \int_{u=0}^L \int_{t=u}^L -\left((\boldsymbol{\omega} - \bar{\boldsymbol{\omega}})^T \boldsymbol{B}\boldsymbol{J}\boldsymbol{\omega}\right)(t) \, (\boldsymbol{\kappa}\boldsymbol{b}' \cdot \boldsymbol{h}_x)(u) \, dt \, du \\ &= \int_{u=0}^L -\left(\int_{t=u}^L (\boldsymbol{\omega} - \bar{\boldsymbol{\omega}})^T \boldsymbol{B}\boldsymbol{J}\boldsymbol{\omega} \, dt \right) (\boldsymbol{\kappa}\boldsymbol{b}' \cdot \boldsymbol{h}_x) \, du \end{aligned} \tag{4.60}$$

By several integration by parts, using Fubini's theorem once and supposing that the terms

vanishes at $s = 0$ and $s = L$:

$$\begin{aligned}
\mathcal{B} + \mathcal{C} &= \int_{t=0}^{L} \left((\boldsymbol{\omega} - \bar{\boldsymbol{\omega}})^T \boldsymbol{B}\boldsymbol{J}\boldsymbol{\omega}\boldsymbol{\kappa}\boldsymbol{b} - \left(\int_{u=t}^{L} (\boldsymbol{\omega} - \bar{\boldsymbol{\omega}})^T \boldsymbol{B}\boldsymbol{J}\boldsymbol{\omega}\, du \right) \boldsymbol{\kappa}\boldsymbol{b}' \right) \cdot \boldsymbol{h}_x \, dt \\
&= \int_{t=0}^{L} \left(- \left(\int_{u=t}^{L} (\boldsymbol{\omega} - \bar{\boldsymbol{\omega}})^T \boldsymbol{B}\boldsymbol{J}\boldsymbol{\omega}\, du \right)' \boldsymbol{\kappa}\boldsymbol{b} - \left(\int_{u=t}^{L} (\boldsymbol{\omega} - \bar{\boldsymbol{\omega}})^T \boldsymbol{B}\boldsymbol{J}\boldsymbol{\omega}\, du \right) \boldsymbol{\kappa}\boldsymbol{b}' \right) \cdot \boldsymbol{h}_x \, dt \\
&= \int_{t=0}^{L} \left(- \left(\int_{u=t}^{L} (\boldsymbol{\omega} - \bar{\boldsymbol{\omega}})^T \boldsymbol{B}\boldsymbol{J}\boldsymbol{\omega}\, du \right) \boldsymbol{\kappa}\boldsymbol{b} \right)' \cdot \boldsymbol{h}_x \, dt
\end{aligned} \tag{4.61}$$

Which can be rewritted using the quasi-static hypothesis :

$$\begin{aligned}
\mathcal{B} + \mathcal{C} &= \int_{t=0}^{L} \left(- \left(\int_{u=t}^{L} (\boldsymbol{\omega} - \bar{\boldsymbol{\omega}})^T \boldsymbol{B}\boldsymbol{J}\boldsymbol{\omega}\, du \right) \boldsymbol{\kappa}\boldsymbol{b} \right)' \cdot \boldsymbol{h}_x \, dt \\
&= \int_{t=0}^{L} \left(- \left(\int_{u=t}^{L} \beta(\theta' - \bar{\theta}')(\delta_L - \delta_0) - \left(\beta(\theta' - \bar{\theta}')\right)' \, du \right) \boldsymbol{\kappa}\boldsymbol{b} \right)' \cdot \boldsymbol{h}_x \, dt \\
&= \int_{t=0}^{L} \left(- \left(\beta(\theta' - \bar{\theta}')(L) - \left[\beta(\theta' - \bar{\theta}')\right]_t^L \right) \boldsymbol{\kappa}\boldsymbol{b} \right)' \cdot \boldsymbol{h}_x \, dt \\
&= \int_{t=0}^{L} - \left(\beta(\theta' - \bar{\theta}')\boldsymbol{\kappa}\boldsymbol{b}\right)' \cdot \boldsymbol{h}_x \, dt
\end{aligned} \tag{4.62}$$

Finally :

$$\boldsymbol{D}_x \mathcal{E}_b[\boldsymbol{\omega}[\boldsymbol{x}]](s) \cdot \boldsymbol{h}_x = \int_0^L \left(- \left(\boldsymbol{d}_3 \times \boldsymbol{M}'\right)' - \left(\beta(\theta' - \bar{\theta}')\boldsymbol{\kappa}\boldsymbol{b}\right)' \right) \cdot \boldsymbol{h}_x \, dt \tag{4.63}$$

Internal forces

Thus, the internal forces are related to the variation of internal elastic energy as :

$$\langle -\boldsymbol{f}(s), \boldsymbol{h}_x \rangle = \boldsymbol{D}_x \mathcal{E}(s) \cdot \boldsymbol{h}_x = - \int_0^L \left(\left(\boldsymbol{d}_3 \times \boldsymbol{M}'\right)' + \left(\beta(\theta' - \bar{\theta}')\boldsymbol{\kappa}\boldsymbol{b}\right)' \right) \cdot \boldsymbol{h}_x \, dt \tag{4.64}$$

Finally, we can conclude on the expression of the internal forces :

$$\boldsymbol{f}(s) = \left(\boldsymbol{d}_3 \times \boldsymbol{M}'\right)' + \left(\beta(\theta' - \bar{\theta}')\boldsymbol{\kappa}\boldsymbol{b}\right)' \tag{4.65}$$

Remarquer ici que l'expression est purement locale. Elle ne dépend pas du sens de parcours de la poutre, contrairement au raisonnement suivi. Cette différence est notable avec la démarche de B. Audoly. Faire le bilan des bénéfices de l'hypothèse quasi-statique : - expressions rigoureusement vraies à l'équilibre statique - simplification ds le calcul des efforts - rapidité dans le calcul avec des expressions plus simples - il n'est pas forcément intéressant en terme d'algorithmie d'imposer l'hypothèse quasistatique au cours du calcul. Il faudrait faire un bench pour savoir.

On retombe sur les équations de Kirchhoff à un terme manquant pret. Qui exprime la contribution de la variation moment de flexion à cause de la torsion $\tau \boldsymbol{M}$‘. Peut-être que ce terme est finalement d'un ordre supérieur, si l'on suppose une variation lente de la torsion ? Comment comprendre la disparition de ce terme qui semble nécessaire à l'équilibre statique d'un élément de poutre si l'on en croit les équations de Kirchhoff ?

4.9 Conclusion

On retrouve les équations de kirchhoff dynamique où l'on a négligé les forces inertielles de rotation d'un élément de poutre autour de $\boldsymbol{d}_1$ et $\boldsymbol{d}_2$ pour ne garder que la dynamique de rotation de la section autour de la fibre neutre $\boldsymbol{d}_3$.

The shear force acting on the right side of a section is nothing but $\boldsymbol{T} = \int \boldsymbol{f}$:

$$\boldsymbol{T}(s) = \boldsymbol{d}_3 \times \boldsymbol{M}' + Q\boldsymbol{\kappa}\boldsymbol{b} \tag{4.66}$$

The linear momentum acting on the centerline is given by :

$$m(s) = Q' - \boldsymbol{\kappa}\boldsymbol{b} \cdot (\boldsymbol{d}_3 \times \boldsymbol{M}) \tag{4.67}$$

The main hypothesis are :

- Bernoulli : $\boldsymbol{d}_i \cdot \boldsymbol{d}_j = \delta_{ij}$
- Inextensibility : $\|\boldsymbol{d}_3'\| = 1$
- Quasistatic : at each timestep regarding bending motion $m(s) = 0$

4.10 References

[1] F. Tayeb. "Simulation numérique du comportement mécanique non linéaire de gridshells composés de poutres élancées en matériaux composites et de sections quelconques". PhD thesis. 2015.

[2] L. du Peloux, F. Tayeb, B. Lefevre, O. Baverel, and J.-F. Caron. "Formulation of a 4-DoF torsion / bending element for the formfinding of elastic gridshells". In: *Proceedings of the International Association for Shell and Spatial Structures*. August. Amsterdam, 2015, pp. 1–14.

[3] B. Lefevre, F. Tayeb, L. du Peloux, and J.-F. Caron. "A 4-degree-of-freedom Kirchhoff beam model for the modeling of bending–torsion couplings in active-bending structures". In: *International Journal of Space Structures* 32.2 (2017), pp. 69–83.

[4] M. Bergou, M. Wardetzky, S. Robinson, B. Audoly, and E. Grinspun. "Discrete elastic rods". In: *ACM SIGGRAPH* (2008), pp. 1–12.

[5] M. Bergou, B. Audoly, E. Vouga, M. Wardetzky, and E. Grinspun. "Discrete viscous threads". In: *ACM Transactions on ...* (2010), pp. 1–10.

[6] S. Nabaei. "Mechanical form-finding of timber fabric structures". PhD thesis. EPFL, 2014.

[7] J. Spillmann and M. Teschner. "CORDE : Cosserat Rod Elements for the Dynamic Simulation of One-Dimensional Elastic Objects". In: *Eurographics/ ACM SIGGRAPH Symposium on Computer Animation* (2007), pp. 1–10.

[8] F. B. Fuller. "Decomposition of the linking number of a closed ribbon : A problem from molecular biology". In: 75.8 (1978), pp. 3557–3561.

[9] R. de Vries. "Evaluating changes of writhe in computer simulations of supercoiled DNA". In: *The Journal of Chemical Physics* 122.6 (2005).

[10] R. Vauquelin. "Writhing Geometry at Finite Temperature : Random Walks and Geometric phases for Stiff Polymers". In: 1 (2000).

[11] M. Berger. "Topological Quantities: Calculating Winding, Writhing, Linking, and Higher order Invariants". In: *Lecture Notes in Mathematics* 1973 (2009), pp. 75–97.

[12] P. Jung, S. Leyendecker, J. Linn, and M. Ortiz. "A discrete mechanics approach to the Cosserat rod theory—Part 1: static equilibria". eng. In: *International journal for numerical methods in engineering* 85.1 (2010), pp. 31–60.

[13] B. Audoly, M. Amar, and Y. Pomeau. *Elasticity and geometry*. 2010, p. 600.

[14] R. Bishop. "There is more than one way to frame a curve". In: *Mathematical Association of America* (1975).

[15] S. Adriaenssens, M. Barnes, and C. Williams. "A new analytic and numerical basis for the form-finding and analysis of spline and gridshell structures". In: *Computing Developments in Civil and Structural Engineering*. Ed. by B. Kumar and B. H. V. Topping. Edinburgh: Civil-Comp Press, 1999, pp. 83–91.